



# Internal Capillary-Gravity Wilton Ripples

Benjamin F. Akers<sup>1</sup> · David M. Ambrose<sup>2</sup>

Received: 27 June 2024 / Accepted: 21 January 2025  
© The Author(s) 2025

## Abstract

Periodic traveling waves at the interface of two incompressible, inviscid fluids subject to gravity and surface tension are studied. We focus on the case in which the linearization about the quiescent state has a two-dimensional kernel. We prove the existence of sheets of traveling waves in this circumstance. We also compute Wilton ripples in which the leading term has a (1:2) harmonic resonance, the triad ripple configuration. Global branches of waves are computed, terminating in three types of self-intersecting waves.

**Keywords** Traveling waves · Vortex sheets · Wilton ripples · Lyapunov–Schmidt decomposition

## 1 Introduction

We study the question of existence of spatially periodic traveling waves at the interface between two irrotational, incompressible, immiscible fluids. The interface divides  $\mathbb{R}^2$  into two regions, with the upper region occupied by the upper fluid and the lower region occupied by the lower fluid. The fluids are each of infinite vertical extent, and we consider the horizontally periodic case. Each fluid has its own constant density; these densities are non-negative and not both zero. If one density equals zero then this is the single-fluid case, for which all of our results also apply. In the single-fluid case, the boundary curve is not an “interface” per se, but we will still describe the free fluid boundary as an interface throughout the work, for convenience. The interface height may be multi-valued, i.e., we do not restrict to the case in which the curve separating the two fluid regions is a graph with respect to the horizontal coordinate. The fluid velocity in each phase is subject to the Euler equations, accounting for the effects of

---

✉ David M. Ambrose  
dma68@drexel.edu

Benjamin F. Akers  
benjamin.akers@afit.edu

<sup>1</sup> Department of Mathematics and Statistics, Air Force Institute of Technology, WPAFB, OH 45433, USA

<sup>2</sup> Department of Mathematics, Drexel University, Philadelphia, PA 19104, USA

gravity and surface tension. In this setting, we both prove that traveling waves exist as well as compute them. In the present work we focus on the case in which the linearized equations of motion have a two-dimensional kernel; the one-dimensional case has been treated previously by the authors and collaborators in [4, 12].

We utilize a traveling wave formulation in which the height of the interface is not assumed to be single-valued; this framework was developed by the authors and Wright in [1]. This formulation will be detailed in Sect. 2 below, but we now describe it briefly. The usual traveling wave formulation for a function  $f$ , say, is to make the ansatz that  $f(x - ct)$  is a solution of the evolution equation under consideration. We do not use this ansatz, and instead consider a parameterized curve  $(x, y)$  traveling with velocity  $(c, 0)$ , so that  $(x, y)_t = (c, 0)$ . We then need a second equation to complete the traveling wave ansatz, and we do this by taking another time derivative of this equation. Other authors have treated the possibility of waves with multi-valued height in two-dimensional fluids by means of a conformal mapping [17, 28], for example. The present approach, however, has the advantage that it is amenable to three-dimensional problems as well [8, 9].

In addition to its use in the above-mentioned works, the authors and Wright used this formulation for the extension of the theory of Crapper waves (which are pure capillary waves) to allow for small effects of gravity [7]. The authors and Sulon have also used this formulation for the study of interfacial periodic traveling waves in the presence of hydroelastic effects [5, 6]. Of these papers, the most similar to the current works are [12] and [6]. In [12], the traveling wave equations for the system being studied at present were developed. It was shown there that the kernel of the linearized operator is always either one-dimensional or two-dimensional. Existence of traveling waves in the case of one-dimensional kernels was developed there by use of an “identity-plus-compact” form of a global bifurcation theorem. The paper [5] extended this theory for the one-dimensional kernel case to the presence of hydroelastic effects, as in the models developed by Plotnikov and Toland [26].

The most interesting case of traveling waves originating from a two-dimensional kernel are the Wilton ripples. The existence and character of ripples has been studied in a variety of contexts. In a family of weakly nonlinear models, resonant Wilton ripples have been shown to exist and be parametrically analytic in amplitude [2, 3]. Branches of traveling ripples when the linearization about the flat state has two dimensional kernel have been shown to exist in the Whitham equation [19, 24]. In the water wave problem, Wilton ripples have been shown to exist in the presence of vorticity [25]. While most studies of the resonant case focus on the triad ripple, higher frequency ripples have been computed [23]. Gravity-capillary ripples have been calculated in the presence of magnetic fields [30]. Resonant triad ripples have been computed in a two-fluid internal wave system absent surface tension but with two free boundaries [27]. Triad resonances in the gravity-capillary problem have also been used to generalize Wilton ripples to three dimensions [16].

The proof of existence of traveling waves with two-dimensional kernels in the present work follows the arguments of the prior work of the authors and Sulon [6]. There, a two-dimensional family of waves was found to exist, with the parameters taken to be the wave speed and the surface tension coefficient. In the hydroelastic setting of [6], this surface tension parameter was a lower-order parameter, as surface tension

arises in the evolution equations as a second-derivative term while the leading-order hydroelastic term has four derivatives. We again use the surface tension coefficient as the second parameter; thus, a difference with the prior work is that in this case, this bifurcation parameter corresponds to the leading-order term of the evolution equations. As in [6], the case of two-dimensional kernels further subdivides into two more cases, those of non-resonant wave interactions and the resonant case. In both cases we make a Lyapunov–Schmidt decomposition and apply the implicit function theorem first to the resulting infinite-dimensional system and then to the remaining finite-dimensional system. In analyzing the finite-dimensional systems we follow ideas of the works [15] and [18]. This is especially relevant for the resonant case, as we study the two-dimensional system in polar coordinates, as in [18].

In our numerical results, we find the Wilton ripples originating from a two-dimensional kernel in the resonant case, with both the surface tension coefficient and the spatial period of the wave held constant. In our analytical results, while we do treat the resonant case of the two-dimensional kernel, our surface tension coefficient is allowed to vary, as in the prior works [6, 18]. Other prior analytical work allowed the spatial period to vary [19]. Allowing variations in the surface tension or spatial period in some ways ameliorates the worst of the resonance; specifically, the Wilton ripples occur at specific values of the Bond number, and by varying the surface tension or the spatial period, the Bond number is changed from the most strongly resonant situation.

The plan of the paper is as follows. In Sect. 2, we give the traveling wave formulation for a parameterized interface. In Sect. 3, we state our main theorem (Theorem 4) and we prove it; this includes both the non-resonant and resonant cases. We present our computational results in Sect. 4. We briefly give some concluding remarks in Sect. 5. Finally, Appendix A and Appendix B give some calculations needed for the proofs of Sect. 3.

## 2 Equations of Motion and Formulation

We consider a parameterized curve  $(x(\alpha, t), y(\alpha, t))$  which is the interface at time  $t$  between the upper and lower fluids. Each fluid is of infinite vertical extent. The curve is horizontally periodic, meaning that for a fixed  $M > 0$ , we have

$$x(\alpha + 2\pi, t) = x(\alpha, t) + M, \quad y(\alpha + 2\pi, t) = y(\alpha, t),$$

for all  $\alpha$  and all  $t$ . Rather than consider the curve  $(x, y)$  directly, we will frequently work with the tangent angle,  $\theta(\alpha, t)$ , that the curve forms with the horizontal. This is defined as  $\theta = \tan^{-1}(y_\alpha/x_\alpha)$ . The parameter,  $\alpha$ , along the curve can be chosen in a variety of ways, and we will take a normalized arclength parameterization. This means that we will take  $\alpha$  proportional to arclength, with  $\alpha \in [0, 2\pi]$ . The length of one period of the curve will be  $L(t)$ , so that if  $s$  denotes arclength, then  $s_\alpha(\alpha, t) = s_\alpha(t) = L(t)/2\pi$ . The curve is taken to have normal and tangential velocities  $U$  and  $V$ , respectively, so that

$$(x, y)_t = U\hat{\mathbf{n}} + V\hat{\mathbf{t}}, \tag{1}$$

where  $\hat{\mathbf{n}}$  and  $\hat{\mathbf{t}}$  are the usual frame of normal and tangential vectors, respectively, i.e.,

$$\hat{\mathbf{t}} = \frac{(x_\alpha, y_\alpha)}{s_\alpha}, \quad \hat{\mathbf{n}} = \frac{(-y_\alpha, x_\alpha)}{s_\alpha}.$$

The normal velocity,  $U$ , is determined from the fluid dynamics, and specifically will be the normal component of the Birkhoff–Rott integral. The tangential velocity,  $V$ , will be chosen to enforce our normalized arclength parameterization.

More specifically, if we complexify the position of the curve  $(x, y)$  as  $z(\alpha, t) = x(\alpha, t) + iy(\alpha, t)$ , then the Birkhoff–Rott integral is  $\mathbf{W} = (W_1, W_2)$ , which satisfies

$$W_1 - iW_2 := B[z]\gamma = \frac{1}{2iM} \text{PV} \int_0^{2\pi} \gamma(\alpha', t) \cot\left(\frac{1}{2}(z(\alpha, t) - z(\alpha', t))\right) d\alpha'.$$

The normal velocity is then  $U = \mathbf{W} \cdot \hat{\mathbf{n}}$ . The function  $\gamma(\alpha, t)$  appearing inside the Birkhoff–Rott integral is the vortex sheet strength, and is the derivative with respect to  $\alpha$  of the jump in velocity potential across the free surface. As such,  $\gamma$  encodes much of the information about the fluid velocity; indeed, knowing  $\gamma$  and the interface position  $(x, y)$  is enough information to allow the fluid velocity field to be reconstructed everywhere. The evolution equation for  $\gamma$  can be found by considering the Bernoulli equation for the velocity potential in the interior of each fluid region and taking the jump across the interface, as in [14]. Full details of the calculation can be found there or in [11], and the result is the equation

$$\begin{aligned} \gamma_t = & \frac{\tau\theta_{\alpha\alpha}}{|z_\alpha|} + \frac{((V - \mathbf{W} \cdot \hat{\mathbf{t}})\gamma)_\alpha}{|z_\alpha|} \\ & - 2A \left( \frac{\mathbf{W}_t \cdot \hat{\mathbf{t}}}{|z_\alpha|} + \frac{1}{8} \frac{(\gamma^2)_\alpha}{|z_\alpha|^2} + gy_\alpha - (V - \mathbf{W} \cdot \hat{\mathbf{t}})(\mathbf{W}_\alpha \cdot \hat{\mathbf{t}}) \right). \end{aligned} \quad (2)$$

The parameters are  $\tau$ , the positive coefficient of surface tension, the constant acceleration due to gravity,  $g$ , and the Atwood ratio,  $A = \frac{\rho_1 - \rho_2}{\rho_1 + \rho_2}$ . Here,  $\rho_1$  and  $\rho_2$  are the constant densities of the lower and upper fluid, respectively. If  $A = 1$  or  $A = -1$ , this indicates the absence of one of the fluids; the theory still applies in this case, but the boundary curve is not an interface but instead is just the boundary of the one fluid which is present.

The tangential velocity,  $V$ , is found by differentiating the equation  $s_\alpha = L(t)/2\pi$  with respect to time. As in any of the prior works by the authors and collaborators such as [5], inspired by the work of Hou, Lowengrub, and Shelley [21, 22], this implies that the tangential velocity satisfies

$$V_\alpha(\alpha, t) = \theta_\alpha U - \frac{1}{2\pi} \int_0^{2\pi} \theta_\alpha U d\alpha. \quad (3)$$

The tangential velocity,  $V$ , then, may be taken as any antiderivative of this. We will specify a specific antiderivative shortly.

A typical traveling wave formulation is to declare the unknowns to be functions of the horizontal spatial variable adjusted for a translation in time. However, our unknowns are not functions of the horizontal spatial variable but are rather functions of the normalized arclength,  $\alpha$ . We instead use the traveling wave ansatz as introduced in [1] and further developed in [12]. If we let  $c \in \mathbb{R}$  be the speed of the traveling wave, then our development of the traveling wave equations for a parameterized curve begins from the equation

$$(x, y)_t = (c, 0). \quad (4)$$

We note that (4) is clearly a traveling wave ansatz, in that it specifies that a curve,  $(x, y)$ , translates rigidly with speed  $c$ . It also fixes parameterization, in that a point at time  $(x(\alpha, 0), y(\alpha, 0))$  on the curve at time zero will at other times be at the position  $(x(\alpha, t) + ct, y(\alpha, t))$ ; thus, we are specifying that all of the points on the curve also are translating with speed  $c$ . Of course, using a Lagrangian parameterization which tracks material points, one would not expect the individual material points to all move with the wave speed. However, we are using an artificial tangential velocity,  $V$ , which keeps the curve parameterized by arclength at all times. This choice of tangential velocity also fixes the parameterization so that all points on the curve translate with the wave speed.

Substituting (1) into (4) yields the following system of equations:

$$\begin{aligned} -U \sin(\theta) + V \cos(\theta) &= c, \\ U \cos(\theta) + V \sin(\theta) &= 0. \end{aligned}$$

The solution of these equations is

$$U = -c \sin(\theta), \quad (5)$$

as well as  $V = c \cos(\theta)$ . In light of the normalized arclength parameterization requirement (3), however, these two equations are redundant. That is, if we have  $U = -c \sin(\theta)$ , then

$$\theta_\alpha U = -c \theta_\alpha \sin(\theta) = \partial_\alpha (c \cos(\theta)) = V_\alpha.$$

Notice that since  $\theta_\alpha U$  is the derivative of a periodic function, it has zero mean, and thus (3) is satisfied.

To complete the traveling wave formulation, we still need a second equation. That is, if we find a curve  $(x, y)$  and vortex sheet strength  $\gamma$  which satisfy (5) at an instant, it may not be satisfied at subsequent times. Thus we also differentiate (5) with respect to time, requiring

$$U_t = -c \theta_t \cos(\theta).$$

Since the traveling wave is of permanent form, however, we have  $\theta_t = 0$ . Using the definition of  $U$  as  $U = \mathbf{W} \cdot \hat{\mathbf{n}}$ , and again the fact that  $\hat{\mathbf{n}}_t = 0$  because the wave is of

permanent form, we find

$$U_t = \mathbf{W}_t \cdot \hat{\mathbf{n}} = 0. \quad (6)$$

Using the complexified form of  $\mathbf{W}$ , and using that  $z_t(\alpha, t) = z_t(\alpha', t) = c$ , we see that (6) can be expressed as

$$\begin{aligned} U_t = \mathbf{W}_t \cdot \hat{\mathbf{n}} &= \operatorname{Re} \left\{ (W_1 - iW_2)_t \left( \frac{iz_\alpha}{s_\alpha} \right) \right\} \\ &= \operatorname{Re} \left\{ \frac{z_\alpha}{2ms_\alpha} \operatorname{PV} \int_0^{2\pi} \gamma_t(\alpha', t) \cot \left( \frac{1}{2}(z(\alpha, t) - z(\alpha', t)) \right) d\alpha' \right\} = 0. \end{aligned}$$

We show in [12] that this is satisfied if and only if

$$\gamma_t = 0. \quad (7)$$

To summarize our formulation so far, we state the following proposition proved in [12].

- Proposition 1** (i) *Suppose that  $(x(\alpha, t), y(\alpha, t))$  and  $\gamma(\alpha, t)$  solve (1), (2), and moreover there exists  $c \in \mathbb{R}$  such that (5), (7) are satisfied, for all  $\alpha$  and  $t$ . Then  $(x(\alpha, t), y(\alpha, t))$  and  $\gamma(\alpha, t)$  constitute a traveling wave solution with speed  $c$ .*  
 (ii) *If  $(\check{x}, \check{y})$  and  $\check{\gamma}$  constitute a traveling wave solution with speed  $c$  of (1), (2), then there exists a reparameterization which maps  $((\check{x}, \check{y}), \check{\gamma}) \mapsto ((x, y), \gamma)$ , where  $(x(\alpha, t), y(\alpha, t))$  and  $\gamma(\alpha, t)$  satisfy (5), (7) for all  $\alpha$  and  $t$ .*

In principle, therefore, our traveling wave formulation is (5), (7). However we need to further develop these equations before using them analytically.

We will be reconstructing the curve,  $z$ , from its tangent angle. If we knew that  $\theta$  is the tangent angle associated to the curve  $z$ , we would have that  $z_\alpha = s_\alpha e^{i\theta}$ , and we could then find  $z$  by taking the antiderivative of this. We define the average values

$$\overline{\cos(\theta)} = \frac{1}{2\pi} \int_0^{2\pi} \cos(\theta(\beta)) d\beta, \quad \overline{\sin(\theta)} = \frac{1}{2\pi} \int_0^{2\pi} \sin(\theta(\beta)) d\beta.$$

Integrating  $z_\alpha = s_\alpha e^{i\theta}$  over one period, and using our periodicity assumptions, we would have

$$M = z(2\pi, t) - z(0, t) = \int_0^{2\pi} z_\alpha(\alpha, t) d\alpha = s_\alpha \int_0^{2\pi} \cos(\theta) + i \sin(\theta) d\alpha.$$

Therefore, we see that ideally,

$$s_\alpha = \frac{M}{2\pi \overline{\cos(\theta)}}, \quad \overline{\sin(\theta)} = 0.$$

Unfortunately not all  $2\pi$ -periodic tangent angles give rise to an appropriately periodic curve. As such, when reconstructing a curve from  $\theta$ , we need to introduce corrections. To this end, assuming  $\overline{\cos(\theta)} \neq 0$ , we introduce a curve associated to  $\theta$ , which we call  $\tilde{Z}$  :

$$\tilde{Z}[\theta](\alpha) = \frac{M}{2\pi \overline{\cos(\theta)}} \left( \int_0^\alpha e^{i\theta(\beta)} d\beta - i\alpha \overline{\sin(\theta)} \right),$$

This curve,  $\tilde{Z}[\theta]$ , then, does satisfy our periodicity assumption,

$$\tilde{Z}[\theta](\alpha + 2\pi, t) = \tilde{Z}[\theta](\alpha, t) + M,$$

for all  $\alpha$  and  $t$ . The normal and tangent vectors,  $\tilde{T}$  and  $\tilde{N}$ , to this curve  $\tilde{Z}[\theta]$ , are

$$\tilde{T}[\theta] = \frac{\partial_\alpha \tilde{Z}[\theta]}{|\partial_\alpha \tilde{Z}[\theta]|}, \quad \tilde{N}[\theta] = \frac{i \partial_\alpha \tilde{Z}[\theta]}{|\partial_\alpha \tilde{Z}[\theta]|}.$$

Note that if  $\overline{\sin(\theta)} = 0$ , then we have  $\tilde{T}[\theta] = e^{i\theta}$  and  $\tilde{N}[\theta] = ie^{i\theta}$ .

Since the mean of  $\gamma$  is constant through the evolution, we decompose  $\gamma$  as  $\gamma = \bar{\gamma} + \gamma_1$ , with  $\bar{\gamma}$  constant and with the mean of  $\gamma_1$  equal to zero. We also at this time introduce the periodic Hilbert transform,

$$Hf(\alpha) = \frac{1}{2\pi} \text{PV} \int_0^{2\pi} f(\alpha') \cot\left(\frac{1}{2}(\alpha - \alpha')\right) d\alpha'.$$

Two relevant properties of the Hilbert transform are that for any constant  $d$ , we have  $Hd = 0$ , and if  $f$  is a periodic function with mean zero, then  $H^2 f = -f$ . The relevance of the Hilbert transform for the problem under consideration is that the Birkhoff–Rott integral can be well-approximated by an appropriate Hilbert transform. We introduce an operator  $K[z]$  which will be the remainder from making this approximation; the definition of  $K[z]$  is

$$K[z]f(\alpha) = B[z]f(\alpha) - \frac{1}{2iz_\alpha(\alpha)} Hf(\alpha). \quad (8)$$

If we determine  $\mathbf{W}$  and  $\hat{\mathbf{n}}$  from  $\tilde{Z}$ , then (5) becomes

$$\text{Re} \left\{ B[\tilde{Z}[\theta]](\gamma) \tilde{N}[\theta] \right\} = -c \sin(\theta).$$

Further rewriting this equation using  $\gamma = \bar{\gamma} + \gamma_1$  and also using (8) yields

$$H\gamma_1 + 2|\partial_\alpha \tilde{Z}[\theta]| \text{Re} \left\{ (K[\tilde{Z}](\bar{\gamma} + \gamma_1)) \tilde{N}[\theta] \right\} + 2c|\partial_\alpha \tilde{Z}[\theta]| \sin(\theta) = 0. \quad (9)$$

Applying the Hilbert transform to (9), and substituting  $\theta = \Theta(\theta, \gamma_1; c)$  (with  $\Theta$  to be defined), we find the equation  $\gamma_1 - \Gamma(\theta, \gamma_1; c) = 0$ , where

$$\begin{aligned} & \Gamma(\theta, \gamma_1; c) \\ &= 2H \left( |\partial_\alpha \tilde{Z}[\Theta(\theta, \gamma_1; c)]| \operatorname{Re} \left\{ (K[\tilde{Z}[\Theta(\theta, \gamma_1; c)]](\bar{\gamma} + \gamma_1)) \tilde{N}[\Theta(\theta, \gamma_1; c)] \right\} \right. \\ & \quad \left. + c |\partial_\alpha \tilde{Z}[\Theta(\theta, \gamma_1; c)]| \sin(\Theta(\theta, \gamma_1; c)) \right). \end{aligned}$$

After these considerations, the equation  $\gamma_t = 0$  becomes  $\tau(\theta_{\alpha\alpha} + \tilde{\Phi}) = 0$ , where

$$\begin{aligned} \tilde{\Phi}(\theta, \gamma; c) &= \frac{1}{\tau} \partial_\alpha ((c \cos(\theta) - \operatorname{Re}(B[\tilde{Z}[\theta]]\gamma\tilde{T}[\theta]))\gamma) \\ & \quad - \frac{A}{\tau} \left( \frac{\pi \cos(\theta)}{2M} \partial_\alpha (\gamma^2) + \frac{gM}{\pi \cos(\theta)} (\sin(\theta) - \overline{\sin(\theta)}) \right) \\ & \quad + \frac{M}{2\pi \cos(\theta)} \partial_\alpha \left( (c \cos(\theta) - \operatorname{Re}\{B[\tilde{Z}[\theta]]\gamma\tilde{T}[\theta]\}) \right). \end{aligned}$$

Before defining our final operator for the  $\theta$  equation, we must introduce an inverse derivative operator. We define  $\partial_\alpha^{-1}$  to be the mean zero antiderivative which acts on mean zero periodic functions. For a mean zero periodic function  $f$  with Fourier series

$$f(\alpha) = \sum_{k \neq 0} \hat{f}(k) e^{ik\alpha},$$

we define  $\partial_\alpha^{-1} f$  to be

$$\partial_\alpha^{-1} f = \sum_{k \neq 0} \frac{\hat{f}(k)}{ik} e^{ik\alpha}.$$

With this in mind, we define the mapping  $\Theta$  by

$$\Theta(\theta, \gamma_1; c) = -\partial_\alpha^{-2} \tilde{\Phi}(\theta, \bar{\gamma} + \gamma_1; c),$$

where we observe that our application of  $\partial_\alpha^{-2}$  is valid because  $\tilde{\Phi}$  does indeed have mean zero. Our final traveling wave formulation is then

$$\theta - \Theta(\theta, \gamma_1; c) = 0, \quad \gamma_1 - \Gamma(\theta, \gamma_1; c) = 0. \quad (10)$$

We let  $\mu = (c, \tau)$ , and then we can restate (10) as

$$F(\theta, \gamma_1; \mu) = 0.$$

We need to know the mapping properties of  $(\Theta, \Gamma)$ . We will work in spatially periodic Sobolev spaces, namely subsets of  $H^1$  and  $H^2$ . The spaces  $H_{\text{even}}^2$  and  $H_{\text{odd}}^2$  denote the subspaces of  $H^2$  of even and odd functions, respectively (i.e., functions with cosine expansions and functions with sine expansions). Furthermore, we let  $\dot{H}_{\text{even}}^2$  be the homogeneous Sobolev  $H^2$  restricted to even functions, which is the same as saying that it is the subspace of  $H_{\text{even}}^2$  consisting of functions with zero mean.

We must address non-self-intersection of solutions as well. We do so by means of a chord-arc condition, which has been used in many works on initial value problems for free-surface flows, such as [10, 29]. We also must have that the mean value of cosine be nonzero. We therefore define the open set  $\mathcal{U}_{b,h}$  to be the subset of  $H^1 \times \dot{H}^1 \times \mathbb{R}$  such that  $(\theta, \gamma_1; c) \in \mathcal{U}_{b,h}$  if and only if  $\theta$  is odd,  $\gamma_1$  is even,  $\overline{\cos(\theta)} > h$ , and  $\tilde{Z}[\theta]$  and  $\tilde{Z}[\Theta(\theta, \gamma_1; c)]$  both satisfy the chord-arc condition,

$$\left| \frac{\tilde{Z}(\beta) - \tilde{Z}(\beta')}{\beta - \beta'} \right| > b, \quad \forall \beta, \beta'.$$

The following result on the mapping properties of  $(\Theta, \Gamma)$  was proved in [12].

**Theorem 2** *For all  $b > 0$  and  $h > 0$ , the pair  $(\Theta, \Gamma)$  is a smooth, compact map from  $\mathcal{U}_{b,h}$  into  $H_{\text{odd}}^2 \times \dot{H}_{\text{even}}^2$ . If  $(\theta, \gamma_1; c)$  solves (10), then  $(\theta, \gamma_1)$  correspond to a spatially periodic, symmetric traveling wave solution of (1), (2) with speed  $c$  and period  $M$ . The position of this traveling wave is given by  $\tilde{Z}[\theta](\alpha) + ct$ , and the vortex sheet strength for this traveling wave is  $\bar{\gamma} + \gamma_1(\alpha)$ .*

### 3 Existence of Traveling Waves via Bifurcation with a Two-Dimensional Kernel

As developed in [12], the linearized mapping is

$$L(c, \tau) \begin{bmatrix} \check{\theta} \\ \check{\gamma} \end{bmatrix} = \begin{bmatrix} \check{\theta} - D\Theta \\ \check{\gamma} - D\Gamma \end{bmatrix} = \begin{bmatrix} L_{11} & L_{12} \\ L_{21} & L_{22} \end{bmatrix} \begin{bmatrix} \check{\theta} \\ \check{\gamma} \end{bmatrix},$$

where the operators  $L_{ij}$  are given by

$$\begin{aligned} L_{11} &= 1 + \frac{\pi \bar{\gamma}}{M} \left( \frac{\bar{\gamma}}{\tau} - \frac{cAM}{\pi \tau} \right) \partial_\alpha^{-1} H - \frac{AgM}{\pi \tau} \partial_\alpha^{-2} \mathbb{P}, \\ L_{12} &= - \left( \frac{A\bar{\gamma}\pi}{\tau M} - \frac{c}{\tau} \right) \partial_\alpha^{-1} \mathbb{P}, \\ L_{21} &= -\bar{\gamma}c \left( \frac{\bar{\gamma}}{\tau} - \frac{cAM}{\pi \tau} \right) \partial_\alpha^{-1} \mathbb{P} - \frac{cM^2 Ag}{\pi^2 \tau} \partial_\alpha^{-2} H, \end{aligned}$$

and

$$L_{22} = 1 - c \left( \frac{A\bar{\gamma}}{\tau} - \frac{cM}{\pi \tau} \right) \partial_\alpha^{-1} H.$$

We can express this spectrally, for  $k \neq 0$ , through the formulas

$$\begin{aligned}\widehat{L}_{11} &= 1 - \frac{\pi \bar{\gamma}}{M} \left( \frac{\bar{\gamma}}{\tau} - \frac{cAM}{\pi \tau} \right) |k|^{-1} + \frac{AgM}{\pi \tau} k^{-2}, \\ \widehat{L}_{12} &= i \left( \frac{A\bar{\gamma}\pi}{\tau M} - \frac{c}{\tau} \right) k^{-1}, \\ \widehat{L}_{21} &= i \bar{\gamma} c \left( \frac{\bar{\gamma}}{\tau} - \frac{cAM}{\pi \tau} \right) k^{-1} - i \frac{cM^2 Ag}{\pi^2 \tau} \cdot \frac{1}{k|k|},\end{aligned}$$

and

$$\widehat{L}_{22} = 1 + c \left( \frac{A\bar{\gamma}}{\tau} - \frac{cM}{\pi \tau} \right) |k|^{-1}.$$

For  $k = 0$ , we have  $\widehat{L}_{ij} = \delta_{ij}$ , i.e., the identity matrix.

Note that  $L(c, \tau)$  is of the form “identity plus compact;” that is, all of the non-identity terms comprising  $L$  involve negative powers of derivatives, and are therefore smoothing and thus compact. More specifically, recall the function spaces used to describe the nonlinear mapping in Theorem 2. In this functional setting, we consider  $L(c, \tau)$  as a bounded linear mapping from  $H_{\text{odd}}^1 \times \dot{H}_{\text{even}}^1$  to  $H_{\text{odd}}^1 \times \dot{H}_{\text{even}}^1$ . Upon subtracting the identity, we see that  $L - I$  is a bounded linear mapping from  $H_{\text{odd}}^1 \times \dot{H}_{\text{even}}^1$  to  $H_{\text{odd}}^2 \times \dot{H}_{\text{even}}^2$ . By Rellich’s theorem, this gain of regularity implies the mapping  $L - I$  is compact. As such,  $L(c, \tau)$  has closed range. We will see below that the kernel of  $L(c, \tau)$  and the kernel of its adjoint are finite-dimensional. This implies then that  $L(c, \tau)$  is Fredholm.

The following proposition on the spectrum of  $L(c, \tau)$  was proved in [12].

**Proposition 3** *The spectrum of*

$$L(c, \tau) : H_{\text{odd}}^1 \times \dot{H}_{\text{even}}^1 \rightarrow H_{\text{odd}}^1 \times \dot{H}_{\text{even}}^1$$

is  $\{1\} \cup \{\lambda_k(c, \tau) : k \in \mathbb{N}\}$ , where

$$\lambda_k(c, \tau) = 1 + \frac{2\bar{\gamma}cAM\pi - M^2c^2 - \bar{\gamma}^2\pi^2}{M\pi\tau} k^{-1} + \frac{gAM}{\pi\tau} k^{-2}.$$

Each eigenvalue of  $L(c, \tau)$  has equal geometric and algebraic multiplicity, which we denote

$$N_\lambda(c, \tau) = \{k \in \mathbb{N} : \lambda_k(c, \tau) = \lambda\}.$$

The associated eigenspace is

$$E_\lambda(c, \tau) = \text{span} \left\{ \left[ \begin{array}{c} -(\pi/cM) \sin(k\alpha) \\ \cos(k\alpha) \end{array} \right] : k \in \mathbb{N} \text{ with } \lambda_k(c, \tau) = \lambda \right\}.$$

Let the polynomial  $R(k; \tau)$  be given by

$$R(k; \tau) = \pi^2 \bar{\gamma}^2 A^2 k^2 + \pi \tau k^3 M - \pi^2 k^2 \bar{\gamma}^2 + k A g M^2. \quad (11)$$

For a given  $k$ , if  $R(k; \tau) \geq 0$ , then the values of  $c \in \mathbb{R}$  for which  $\lambda_k(c, \tau) = 0$  are

$$c_{\pm}(k, \tau) = \frac{\pi \bar{\gamma} A}{M} \pm \frac{1}{k M} \sqrt{R(k; \tau)},$$

and this zero eigenvalue has multiplicity equal to either 1 or 2. For a given  $k$ , the multiplicity is equal to 2 (i.e.,  $N_0(c_{\pm}(k, \tau), \tau) = 2$ ) if and only if the single root  $\ell(k) = \frac{A g M}{\pi \tau k}$  of the affine polynomial

$$p(\ell, k; \tau) = \pi \tau \ell k - A g M \quad (12)$$

is a positive integer not equal to  $k$ .

We will need to define another quantity before proceeding. We let  $Q$  denote this quantity, defined as follows:

$$\begin{aligned} Q(k, \ell, \tau, A, g, M, \bar{\gamma}) \\ = \tau M + \left( \frac{k + \ell}{k \ell} \right) \left( \frac{c^2 M^2}{\pi} + \bar{\gamma}^2 \pi - 2 c M \bar{\gamma} A \right) - \left( \frac{k^2 + \ell k + \ell^2}{k^2 \ell^2} \right) \frac{M^2 A g}{\pi}. \end{aligned} \quad (13)$$

In the following theorem, we will need to assume that the parameters are such that  $Q \neq 0$ . We note that this can sometimes be verified. In particular, for the choices  $k = 1$ ,  $\ell = 2$ ,  $\tau = A$ ,  $g = 1$ ,  $M = 2\pi$ , and  $\bar{\gamma} = 0$ , we have  $Q = 4\pi\tau \neq 0$ . This parameter set includes all the waves computed in the numerical section, thus the theorem applies to all of the computations. Note that  $Q$  is a continuous function of its (continuous) arguments, so if  $Q$  is nonzero at a certain choice of parameter values, it will be nonzero for nearby choices of these arguments as well. So, for example, in the above specific choice of parameters, if we vary  $\bar{\gamma}$  to make  $\bar{\gamma} \neq 0$ , then  $Q$  is still nonzero.

Recall that we consider the operator  $L$  to be a map from  $H_{\text{odd}}^1 \times \dot{H}_{\text{even}}^1$  to itself. In the next theorem, statements about the kernel and range of  $L$ , and of its adjoint, and associated projections, are to be understood in this context.

**Theorem 4** *Define the polynomials  $p$  and  $R$  as in (11) and (12). Let the quantity  $Q$  be as in (13). Let  $b > 0$  and  $h > 0$  be arbitrary, and let  $k$  and  $\ell$  be positive integers such that  $k < \ell$  and such that for some  $\tau_* > 0$ , the following hold:*

- (1)  $p(\ell, k; \tau_*) = 0$ ,
- (2)  $R(k, \tau_*) > 0$ , and
- (3)  $Q(k, \ell, \tau_*, A, g, M, \bar{\gamma}) \neq 0$ .

Given  $\mu_* = (c_{\pm}(k, \tau_*), \tau_*)$ , let

$$\begin{aligned}\mathcal{V} &= \text{Ker}(L(\mu_*)), & \mathcal{R} &= \text{Range}(L(\mu_*)), \\ \mathcal{V}^\dagger &= \text{Ker}(L^\dagger(\mu_*)), & \mathcal{R}^\dagger &= \text{Range}(L^\dagger(\mu_*)).\end{aligned}$$

(Here,  $L^\dagger(c, \tau)$  is the Hermitian adjoint of  $L(c, \tau)$ .) Let  $\Pi_{\mathcal{V}^\dagger}$  and  $\Pi_{\mathcal{R}}$  denote the projections onto the given spaces. Let the basis elements of  $\mathcal{V}$  be given as

$$v_j(\alpha) = \left[ \begin{array}{c} -\frac{\pi}{c_{\pm}(k, \tau_*)M} \sin(j\alpha) \\ \cos(j\alpha) \end{array} \right], \quad j \in \{k, \ell\}.$$

**Non-resonant case.** Suppose  $\frac{\ell}{k} \notin \mathbb{N}$ . There exist a neighborhood  $\mathcal{N}_t \subseteq \mathbb{R}^2$  of  $(0, 0)$ , a neighborhood  $\mathcal{N}_\mu \subseteq \mathbb{R}^2$  of  $\mu_*$ , a neighborhood  $\mathcal{N}_{\mathcal{V}} \subset \mathcal{V}$  of 0, and a neighborhood  $\mathcal{N}_{\mathcal{R}^\dagger} \subseteq \mathcal{R}^\dagger \cap U_{b,h}$  of 0, and there exist smooth functions  $\bar{\mu} : \mathcal{N}_t \rightarrow \mathcal{N}_\mu$  and  $\bar{y} : \mathcal{N}_{\mathcal{V}} \times \mathcal{N}_\mu \rightarrow \mathcal{N}_{\mathcal{R}^\dagger}$ , such that

$$\bar{\mu}(0, 0) = \mu_*,$$

and

$$F(t_1 v_k + t_2 v_\ell + \bar{y}(t_1 v_k + t_2 v_\ell, \bar{\mu}(t_1, t_2)); \bar{\mu}(t_1, t_2)) = 0,$$

for all  $(t_1, t_2) \in \mathcal{N}_t$ .

**Resonant case.** Suppose  $\frac{\ell}{k} \in \mathbb{N}$ . Given  $\delta > 0$ , there exist a neighborhood  $\mathcal{N}_r \subseteq \mathbb{R}^+$  around 0, a neighborhood  $\mathcal{N}_\mu \subseteq \mathbb{R}^2$  around  $\mu_*$ , a neighborhood  $\mathcal{N}_{\mathcal{V}} \subseteq \mathcal{V}$  of 0, and a neighborhood  $\mathcal{N}_{\mathcal{R}^\dagger} \subseteq \mathcal{R}^\dagger \cap U_{b,h}$  of 0, and there exist smooth functions  $\bar{\mu} : \mathcal{N}_r \times ((\delta, \pi - \delta) \cup (-\pi + \delta, -\delta)) \rightarrow \mathcal{N}_\mu$  and  $\bar{y} : \mathcal{N}_{\mathcal{V}} \times \mathcal{N}_\mu \rightarrow \mathcal{N}_{\mathcal{R}^\dagger}$ , such that for all  $\beta$  satisfying  $\delta < |\beta| < \pi - \beta$ , and for all  $r \in \mathcal{N}_r$ ,

$$\bar{\mu}(0, \beta) = \mu_*,$$

and

$$F(r \cos(\beta) v_k + r \sin(\beta) v_\ell + \bar{y}(r \cos(\beta) v_k + r \sin(\beta) v_\ell, \bar{\mu}(r, \beta)); \bar{\mu}(r, \beta)) = 0.$$

**Proof** By Proposition 3, the kernel of  $L(\mu)$  is two-dimensional at  $\mu = \mu_*$ . We have noted above that  $L(\mu)$  is a Fredholm operator, and thus we may make the decompositions

$$X = \mathcal{V}^\dagger \oplus \mathcal{R}, \quad U_{b,h} = \mathcal{V} \oplus (\mathcal{R}^\dagger \cap U_{b,h}).$$

For each  $w \in U_{b,h}$ , we therefore may decompose  $w$  as

$$w = v + y,$$

with  $v \in \mathcal{V}$  and  $y \in \mathcal{R}^\dagger \cap U_{b,h}$ . As we are attempting to solve the problem

$$F(w; \mu) = 0,$$

we see that we may equivalently solve the system

$$\Pi_{\mathcal{V}^\dagger} F(v + y; \mu) = 0, \quad (14)$$

$$\Pi_{\mathcal{R}} F(v + y; \mu) = 0. \quad (15)$$

We begin by considering the solvability of (15). We let  $G : \mathcal{V} \times \mathcal{R}^\dagger \rightarrow \mathcal{R}$  be the mapping given by  $G(v, y) = \Pi_{\mathcal{R}} F(v + y; \mu_*)$ . Denoting the Frechet derivative of  $G$  with respect to  $y$  as  $G_y$ , we have  $G_y(0, 0) = \Pi_{\mathcal{R}} L(\mu_*)$ . For any  $y \in \mathcal{R}^\dagger \cap U_{b,h}$ , we have  $G_y(0, 0)y = \Pi_{\mathcal{R}} L(\mu_*)y = L(\mu_*)y$ , since  $L(\mu_*)y$  is of course in the range of  $L(\mu_*)$ . Thus  $G_y(0, 0)$  is surjective onto  $\mathcal{R}$ . Furthermore, for any nonzero  $y \in \mathcal{R}^\dagger \cap U_{b,h}$ , we have that  $y \notin \mathcal{V} = \ker(L(\mu_*))$ , and thus  $G_y(0, 0)y = L(\mu_*)y \neq 0$ . Thus we see that  $G_y(0, 0)$  is also injective.

Since  $G(0, 0) = 0$ , we apply the implicit function theorem to  $G$ , finding the existence of neighborhoods  $\mathcal{N}_{\mathcal{V}}$  of  $0 \in \mathcal{V}$ ,  $\mathcal{N}_\mu$  of  $\mu_* \in \mathbb{R}^2$ , and  $\mathcal{N}_{\mathcal{R}^\dagger}$  of  $0 \in \mathcal{R}^\dagger \cap U_{b,h}$ , and a smooth function  $\bar{y} : \mathcal{N}_{\mathcal{V}} \times \mathcal{N}_\mu \rightarrow \mathcal{N}_{\mathcal{R}^\dagger}$ , such that for all  $(v, \mu) \in \mathcal{N}_{\mathcal{V}} \times \mathcal{N}_\mu$ , we have

$$\Pi_{\mathcal{R}} F(v + \bar{y}(v, \mu); \mu) = 0.$$

This function  $\bar{y}$  satisfies  $\bar{y}(0, \mu) = 0$  for all  $\mu \in \mathcal{N}_\mu$  (since  $\bar{y}$  is unique and since  $F(0, 0; \mu) = 0$  for all  $\mu$ ). This immediately implies that  $\partial_c \bar{y}(0, \mu) = 0$  and  $\partial_\tau \bar{y}(0, \mu) = 0$  for all  $\mu \in \mathcal{N}_\mu$  as well. Finally, we show that  $\bar{y}_v(0, 0)v = 0$  as well. Differentiating  $G(v, \bar{y}(v, \mu)) = 0$  with respect to  $v$  at  $v = 0$ , we find

$$G_v(0, 0)v + G_y(0, 0)\bar{y}_v(0, \mu)v = 0.$$

Since  $G_v(0, 0)v = \Pi_{\mathcal{R}} L(\mu_*)v$  and  $v \in \text{Ker} L(\mu_*)$ , we have that  $G_v(0, 0)v = 0$ . Thus

$$G_y(0, 0)\bar{y}_v(0, \mu)v = 0.$$

Since we have previously established the bijectivity of  $G_y(0, 0)$  and since  $v$  was arbitrary, this implies  $\bar{y}_v(0, \mu) = 0$ .

We next turn to consideration of (14). For any  $v \in \mathcal{V}$ , we may write

$$v(\alpha) = t_1 \left[ -\frac{\pi}{c_\pm(k, \tau_*)M} \frac{\sin(k\alpha)}{\cos(k\alpha)} \right] + t_2 \left[ -\frac{\pi}{c_\pm(k, \tau_*)M} \frac{\sin(\ell\alpha)}{\cos(\ell\alpha)} \right] = t_1 v_1 + t_2 v_2.$$

We thus may represent  $v \in \mathcal{V}$  with a pair  $(t_1, t_2) \in \mathbb{R}^2$ . With this in mind, we define

$$\Phi(t_1, t_2, \mu) = \Pi_{\mathcal{V}^\dagger} F(v + \bar{y}(v, \mu); \mu).$$

Inspection of the formula for  $L(\mu_*)$  indicates that its adjoint  $L^\dagger(\mu_*)$  also has a two-dimensional kernel, with one basis element in wavenumber  $k$  and one basis element in wavenumber  $\ell$ ; we denote these basis elements as  $\phi_k(\cdot, \mu_*)$  and  $\phi_\ell(\cdot, \mu_*)$ . See Appendix A for the detailed expression for these basis elements. We then let  $\Pi_k$  be the projection onto  $\phi_k$  and  $\Pi_\ell$  be the projection onto  $\phi_\ell$ . To solve  $\Phi(t_1, t_2, \mu) = 0$  then is equivalent to solving the system

$$\begin{aligned}\Phi_k(t_1, t_2, \mu) &= \Pi_k \Phi(t_1, t_2, \mu) = 0, \\ \Phi_\ell(t_1, t_2, \mu) &= \Pi_\ell \Phi(t_1, t_2, \mu) = 0.\end{aligned}$$

We can show that for any  $t_2$  and any  $\mu$ , we have  $\Phi_k(0, t_2, \mu) = 0$ . Indeed, so far we have been considering functions with  $2\pi$ -periodicity. If instead we considered  $\frac{2\pi}{\ell}$ -periodicity, we could repeat the above arguments and find the existence of  $\bar{y}_\ell$  such that  $\Pi_{\mathcal{R}_\ell} F(t_2 v_2 + \bar{y}_\ell(t_2 v_2, \mu)) = 0$ , where  $\mathcal{R}_\ell$  is the new range of the linearization. However, as the new set of periodic functions is a subset of the previous set, and since the function  $\bar{y}$  we demonstrated to exist previously was unique, we must have that  $\bar{y}_\ell$  coincides with  $\bar{y}$  when the domain is restricted to  $\frac{2\pi}{\ell}$ -periodic functions. Thus we see that  $t_2 v_2 + \bar{y}(t_2 v_2, \mu)$  is  $\frac{2\pi}{\ell}$ -periodic, as is  $F(t_2 v_2 + \bar{y}(t_2 v_2, \mu))$ . Since  $k < \ell$ , when we project this onto  $\phi_k$  (which, again, is a pair of functions in wavenumber  $k$ ), we get zero. Thus  $\Phi_k(0, t_2, \mu) = 0$ .

In the non-resonant case (so  $\frac{\ell}{k} \notin \mathbb{N}$ ), we also have  $\Phi_\ell(t_1, 0, \mu) = 0$  for all  $t_1$  and  $\mu$ . This condition may not hold in the resonant case, however.

We now define  $\Psi = (\Psi_k, \Psi_\ell)$ , with

$$\begin{aligned}\Psi_k(t_1, t_2, \mu) &= \int_0^1 \partial_{t_1} \Phi_k(x t_1, t_2, \mu) \, dx, \\ \Psi_\ell(t_1, t_2, \mu) &= \int_0^1 \partial_{t_2} \Phi_\ell(t_1, x t_2, \mu) \, dx.\end{aligned}$$

As in [6] and [15], solving  $\Phi_k = \Phi_\ell = 0$  is equivalent to solving  $\Psi_k = \Psi_\ell = 0$ , and furthermore,  $\Psi_k$  and  $\Psi_\ell$  are smooth. We therefore will apply the implicit function theorem to solve

$$0 = \Psi_k(t_1, t_2, \mu) = \Psi_\ell(t_1, t_2, \mu).$$

To apply the implicit function theorem, we want the matrix

$$\begin{bmatrix} \partial_c \Psi_k(0, 0, \mu_*) & \partial_\tau \Psi_k(0, 0, \mu_*) \\ \partial_c \Psi_\ell(0, 0, \mu_*) & \partial_\tau \Psi_\ell(0, 0, \mu_*) \end{bmatrix} \quad (16)$$

to be non-singular. This matrix is equal to

$$\begin{bmatrix} \partial_{t_1, c}^2 \Phi_k(0, 0, \mu_*) & \partial_{t_1, \tau}^2 \Phi_k(0, 0, \mu_*) \\ \partial_{t_2, c}^2 \Phi_\ell(0, 0, \mu_*) & \partial_{t_2, \tau}^2 \Phi_\ell(0, 0, \mu_*) \end{bmatrix}.$$

Since we have established above that  $D\bar{y}(0, \mu) = 0$ , this matrix becomes

$$\begin{bmatrix} \Pi_k \partial_c L(\mu_*) v_1 & \Pi_k \partial_\tau L(\mu_*) v_1 \\ \Pi_\ell \partial_c L(\mu_*) v_2 & \Pi_\ell \partial_\tau L(\mu_*) v_2 \end{bmatrix}. \quad (17)$$

See [6] for full details of the equivalence of the nonsingularity of (16) and (17). What we must show is that the determinant of this matrix is nonzero. Using the formulas developed in Appendix B, we have the following calculation of the determinant of this matrix:

$$\frac{\pi^3}{\langle \phi_k, \phi_k \rangle \langle \phi_\ell, \phi_\ell \rangle} \left( \frac{-A\bar{\gamma}\pi + cM}{cM\tau} \right) (\ell - k) Q(k, \ell, \tau, A, g, M, \bar{\gamma}).$$

The first factor on the right-hand side is clearly positive, and the second is nonzero by assumption (since  $R > 0$ ), the third is nonzero since  $k \neq \ell$ , and the fourth is nonzero by the assumption that  $Q \neq 0$ . Applying the implicit function theorem, we find the neighborhoods  $\mathcal{N}_t$  and  $\mathcal{N}_\mu$ , and the desired function  $\bar{\mu}$ . This completes the proof in the non-resonant case.

We now return to the resonant case. We still have  $\Phi_k(0, t_2, \mu) = 0$  for all  $t_2$  and  $\mu$ , but we may not have  $\Phi_\ell(t_1, 0, \mu) = 0$ . We therefore define alternate auxiliary quantities,  $\tilde{\Psi}_k$  and  $\tilde{\Psi}_\ell$ , and we do so making use of polar coordinates. These new functions are

$$\begin{aligned} \tilde{\Psi}_k(r, \beta, \mu) &= \int_0^1 \partial_{t_1} \Phi_k(xr \cos(\beta), r \sin(\beta), \mu) dx, \\ \tilde{\Psi}_\ell(r, \beta, \mu) &= \int_0^1 \left( \partial_{t_1} \Phi_\ell(xr \cos(\beta), xr \sin(\beta), \mu) \cos(\beta) \right. \\ &\quad \left. + \partial_{t_2} \Phi_\ell(xr \cos(\beta), xr \sin(\beta), \mu) \sin(\beta) \right) dx. \end{aligned}$$

Analogously to the non-resonant case, we wish to solve

$$0 = \tilde{\Psi}_1(r, \beta, \mu) = \tilde{\Psi}_2(r, \beta, \mu),$$

whenever  $r \cos(\beta) \neq 0$ . The functions  $\tilde{\Psi}_k$  and  $\tilde{\Psi}_\ell$  are again smooth, and so we wish to apply the implicit function theorem by demonstrating that the appropriate matrix is nonsingular.

The relevant matrix can be seen to be

$$\begin{bmatrix} \Pi_k \partial_c L(\mu_*) v_k & \Pi_k \partial_\tau L(\mu_*) v_k \\ \sin(\beta) \Pi_\ell \partial_c L(\mu_*) v_\ell & \sin(\beta) \Pi_\ell \partial_\tau L(\mu_*) v_\ell \end{bmatrix}. \quad (18)$$

Again, see [6] for full details as to the equivalence of the nonsingularity of (18) and the analog of (16) for the resonant case. This matrix is non-singular if  $\sin(\beta) \neq 0$  and if the matrix (17) is nonsingular; of course, we have already concluded that under the hypotheses of the current theorem, the matrix (17) is indeed nonsingular. For fixed,

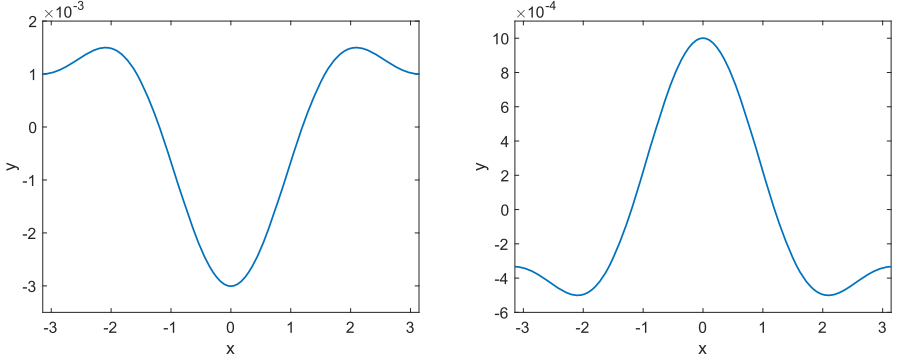


**Fig. 1** Examples of small amplitude Wilton ripple waves with  $\beta = -1$  at  $\tau = 0.5$  (left) and  $\beta = 1$  at  $\tau = 0.1$  (right)

small  $\delta > 0$  and considering the possible set of  $\beta$  as  $[\delta, \pi - \delta] \cup [-\pi + \delta, -\delta]$ , we avoid the possibility of  $\sin(\beta) = 0$ . We again are able to apply the implicit function theorem, resulting in existence of the relevant neighborhoods and the function  $\bar{\mu}$ . This completes the proof of the theorem.  $\square$

## 4 Computations

In addition to establishing the existence of resonant Wilton ripples and non-resonant waves, global branches of Wilton ripples are computed. Such ripples are computed for a discrete sampling of density ratios  $A \in (0, 1)$ . The surface tension is restricted as  $\tau = A$  to ensure a two-dimensional null space in the linearization between wavenumber  $k = 1$  and  $\ell = 2$ , referred to as the triad ripple [2, 3, 23]. The domain width is set at  $M = 2\pi$  and the mean shear  $\bar{\gamma} = 0$ . Small amplitude ripples are asymptotically approximated as

$$\begin{aligned}\theta &= \varepsilon\theta_1 + \varepsilon^2\theta_2 + O(\varepsilon^3), \\ \gamma &= \varepsilon\gamma_1 + \varepsilon^2\gamma_2 + O(\varepsilon^3), \\ c &= c_0 + \varepsilon c_1 + O(\varepsilon^2).\end{aligned}$$

The amplitude scale  $\varepsilon$  is defined to normalize the Fourier coefficient of  $\theta$  at  $k = 1$  so that

$$\theta_1 = \sin(\alpha) + \beta \sin(2\alpha).$$

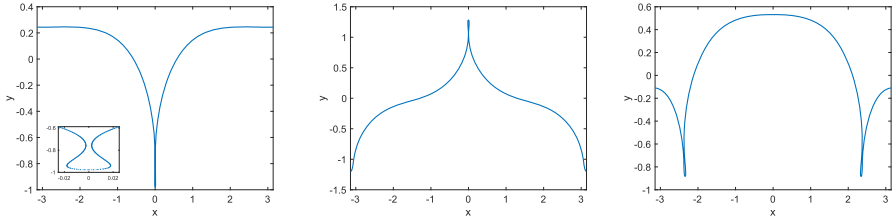


**Fig. 2** Examples of extreme Wilton ripples with  $\beta = -1$  at  $\tau = 0.5$  (left),  $\beta = 1$  at  $\tau = 0.1$  (center), and  $\beta = 1$  at  $\tau = 0.3$  (right). These profiles were computed with  $N_\alpha = 2048$  points per period

Following the same procedure as in [6], the  $O(\varepsilon)$  corrections are computed. The leading order speed correction comes from linear theory,

$$c_0 = \pm \sqrt{\frac{\tau |k|}{2} + \frac{Ag}{|k|}}.$$

The first nonlinear correction gives

$$c_1 = \pm \frac{1}{2} Ac_0^2, \quad \text{and} \quad \beta = \pm 1. \quad (19)$$

The coefficient  $\beta$  is the ratio of the amplitude of the Fourier harmonics at  $k = 1$  and  $\ell = 2$ . This value is used as a switch for the quasi-Newton method, to start the continuation procedure on one branch or the other. Examples of small amplitude waves with both choices of  $\beta$  are in Fig. 1. Note, these waves are computed with fixed surface tension, for which there is only one choice of  $\beta$ . Theorem 4 proves that other choices of  $\beta$  are possible if the surface tension is allowed to vary with amplitude.

The equations of motion are approximated spectrally, using Fourier collocation for the spatial derivatives and an alternating point trapezoid rule for the Birkhoff–Rott integral [13, 20]. The projected equations are then solved via quasi-Newton iteration, as in [1]. The curves are parameterized by pseudo-arclength (i.e., normalized arclength), with  $\alpha \in (0, 2\pi)$  (so that  $\frac{L}{2\pi}\alpha$  is the arclength). The computations presented here used equally spaced points to discretize  $\alpha$ . Small amplitude solutions are computed using the above asymptotics as an initial guess. Larger amplitude solutions are computed via continuation in total displacement,  $h = \max(y) - \min(y)$ .

Global branches of waves, from small amplitude up to a maximal, apparently self-intersecting, wave were computed for  $\tau = A \in (0, 1)$ . Waves are considered to be near self-intersection if the distance between any pair of points is less than 90% of the grid spacing, at which point computations are halted to avoid non-physical self-intersecting profiles. Note, this criteria cannot occur between adjacent points, as the grid spacing is uniform in arclength; it happens only when two non-adjacent grid points approach one another (as in self-intersection). The boundaries of the regions in Fig. 3 where waves are reported to exist are the adaptively computed amplitudes where waves first satisfy the near self-intersection threshold.

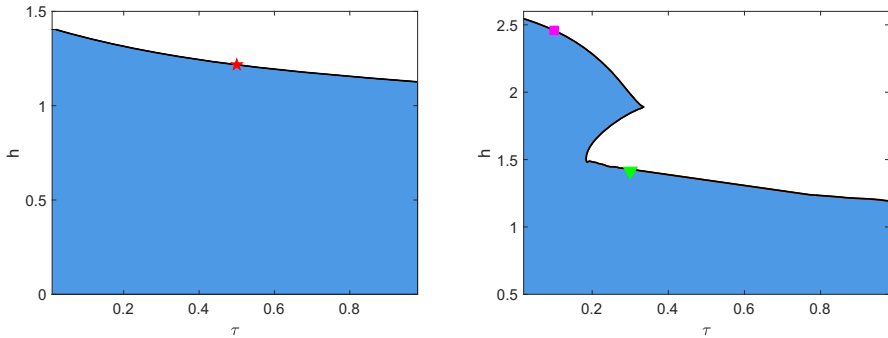


**Fig. 3** Diagrams depicting the regions where traveling resonant triad ripples were computed. Waves were computed in the blue-shaded regions. The left panel depicts triad ripples with  $\beta = -1$ ; the right panel depicts triad ripples with  $\beta = 1$ . The waves in Fig. 2 are marked:  $(\beta = -1, \tau = 0.5)$  with the red star in the left panel,  $(\beta = 1, \tau = 0.1)$  with the magenta square in the right panel, and  $(\beta = 1, \tau = 0.3)$  in the right panel. Examples of small amplitude waves of each type are in Fig. 1

Figure 2 depicts examples of extreme waves. For  $\beta = -1$  the extreme resonant ripple on each branch, at each resonant  $\tau = A \in (0, 1)$ , has a single self-intersecting trough. These waves resemble extreme water waves with surface tension, e.g., the Crapper waves. One such wave is in the left panel of Fig. 2. For  $\beta = 1$  there are two different types of extreme waves. For small  $\tau = A$ , the extreme waves self-intersect at a single crest (as in the center panel of Fig. 2); for large  $\tau = A$ , the extreme waves self-intersect at two separate, symmetric troughs (as in the right panel of Fig. 2). The continuation procedure to compute branches of waves was conducted with  $N_\alpha = 512$  points. Once the near self-intersecting waves were found, the largest wave was interpolated to  $N_\alpha = 2048$  points and recomputed as a resolution check. The differences between the resolutions are indistinguishable at the scale of the figures presented here.

The extreme wave types were explored by computing the regions in the  $\tau h$ -plane in which traveling waves exist, like a phase diagram. For  $\beta = -1$ , the diagram was computed by continuing in  $h$  from small amplitude for each  $\tau$ . The observed extreme wave locations were a monotonic function of  $h$ . In the left panel of Fig. 3, the blue region denotes the  $(h, \tau)$  pairs for which waves with  $\beta = -1$  were computed.

For  $\beta = 1$  there are two qualitatively different extreme waves at which branches of ripples terminate. Moreover the boundary of where waves exist in the  $(h, \tau)$  plane is not a smooth function of  $\tau$ . To trace this boundary, the boundary-tracing continuation procedure developed in [4] was employed. This procedure begins with a single global branch of traveling waves, computed with continuation in amplitude from zero up to the self-intersection threshold. For Fig. 3 the first branch is  $\tau = 0.01$ . Continuation is then employed in both  $h$  and  $\tau$  simultaneously on small circular paths inside the region where waves exist, here counterclockwise, using the extreme wave as the center of the circle. The step angles of this continuation procedure are adaptively chosen; each arc ends at an extreme wave. The location of the new extreme wave is used as the center of the next small circle, the intersection of the previous path and the new circle is used as the initial guess for the first point on the new circle. The radius of the leftmost circle

radius is set to correspond to  $\Delta\tau = 0.01$ , the method adaptively decreases the change in  $\tau$  when necessary ( $\Delta\tau$  decreases to is  $\Delta\tau = 3 \times 10^{-5}$  in the computation of the corners of the boundary in the right panel of Fig. 3.)

This method was employed to trace the boundary of the region in the  $(h, \tau)$  plane where ripples with  $\beta = 1$  exist and is depicted in the right panel of Fig. 3. This boundary appears in three smooth arcs. On the leftmost arc, on which there is marked a single magenta square, the extreme waves self-intersect at a single central peak. On the rightmost arc, marked with a green triangle in Fig. 3, the extreme waves self intersect at two troughs per period. These two arcs are connected by a third arc, where the extreme waves are not near self-intersection. The corners on this boundary are likely the result of a folding of the surface of traveling waves by our projection into the  $(h, \tau)$  plane. The waves above the third arc are observed not to be connected to the flat state for fixed values of  $\tau$  and  $A$ .

## 5 Conclusion

In this work, existence of traveling internal capillary waves which bifurcate from a two dimensional kernel is established. Both the resonant and non-resonant cases are handled. The key step of the existence proof, which employs a Lyapunov–Schmidt decomposition and two uses of the implicit function theorem, requires that a certain matrix must have non-zero determinant. Ripples were also computed for the density ratio/surface tension pairs at which the linear problem has two dimensional kernel. Global branches of traveling ripples were computed, ending in three types of self-intersecting profiles.

## Appendix A: The Kernel of $L^\dagger(\mu_*)$

In this appendix, we carry out some calculations relating to  $L^\dagger(\mu_*)$ . These are used in the proof of the main theorem above.

The adjoint of  $\widehat{L}(\mu)(j)$  is

$$\widehat{L^\dagger(\mu)}(j) = \begin{bmatrix} \Upsilon_{11} & \Upsilon_{12} \\ \Upsilon_{21} & \Upsilon_{22} \end{bmatrix},$$

where the matrix entries are given by

$$\begin{aligned} \Upsilon_{11} &= 1 - \frac{\pi \bar{\gamma}}{M} \left( \frac{\bar{\gamma}}{\tau} - \frac{cAM}{\pi\tau} \right) |k|^{-1} + \frac{AgM}{\pi\tau} k^{-2}, \\ \Upsilon_{12} &= -i\bar{\gamma}c \left( \frac{\bar{\gamma}}{\tau} - \frac{cAM}{\pi\tau} \right) k^{-1} + i \frac{cM^2 Ag}{\pi^2 \tau} \cdot \frac{1}{k|k|}, \\ \Upsilon_{21} &= -i \left( \frac{A\bar{\gamma}\pi}{\tau M} - \frac{c}{\tau} \right) k^{-1}, \end{aligned}$$

$$\Upsilon_{22} = 1 + c \left( \frac{A\bar{\gamma}}{\tau} - \frac{cM}{\pi\tau} \right) |k|^{-1}.$$

Note that this has the same determinant as  $\widehat{L(\mu)}(j)$ , so one of these is singular if and only if the other is. Therefore we see that the kernel of  $L^\dagger(\mu_*)$  has basis elements with wavenumbers  $k$  and  $\ell$  only. Considering  $L^\dagger(\mu_*) \begin{bmatrix} f_1 \\ f_2 \end{bmatrix} = 0$ , we see that (using the equation from the second row of the matrix) that

$$\left( \frac{A\bar{\gamma}\pi}{\tau M} - \frac{c}{\tau} \right) \partial_\alpha^{-1} \mathbb{P} f_1 + \left( 1 - c \left( \frac{A\bar{\gamma}}{\tau} - \frac{cM}{\pi\tau} \right) \partial_\alpha^{-1} H \right) f_2 = 0.$$

We see that we can take  $f_1$  and  $f_2$  as

$$\begin{bmatrix} f_1 \\ f_2 \end{bmatrix} = \begin{bmatrix} (\tau j M + cM \left( \frac{A\bar{\gamma}}{\pi} - \frac{cM}{\pi} \right)) \sin(j\alpha) \\ (-cM + A\bar{\gamma}\pi) \cos(j\alpha) \end{bmatrix}.$$

Note that this is nontrivial, since  $-cM + A\bar{\gamma}\pi$  can be expressed in terms of the polynomial  $R$ , and this is nonzero by assumption. When  $j = k$  we call this vector  $\phi_k$ , and when  $j = \ell$  we call it  $\phi_\ell$ .

## Appendix B: Calculations of Matrix Entries in (17)

We compute the derivatives of  $L(\mu)$  with respect to  $c$  and  $\tau$ , finding

$$\partial_c L(\mu) = \begin{bmatrix} -\frac{\bar{\gamma}A}{\tau} \partial_\alpha^{-1} H & \frac{1}{\tau} \partial_\alpha^{-1} \mathbb{P} \\ \left( -\frac{\bar{\gamma}^2}{\tau} + \frac{2\bar{\gamma}cAM}{\pi\tau} \right) \partial_\alpha^{-1} \mathbb{P} - \frac{M^2 Ag}{\pi^2 \tau} \partial_\alpha^{-2} H & \left( -\frac{A\bar{\gamma}}{\tau} + \frac{2cM}{\pi\tau} \right) \partial_\alpha^{-1} H \end{bmatrix}$$

and

$$\partial_\tau L(\mu) = \begin{bmatrix} -\frac{\pi\bar{\gamma}}{M} \left( \frac{\bar{\gamma}}{\tau^2} - \frac{cAM}{\pi\tau^2} \right) \partial_\alpha^{-1} H + \frac{AgM}{\pi\tau^2} \partial_\alpha^{-2} \mathbb{P} & \left( \frac{A\bar{\gamma}\pi}{\tau^2 M} - \frac{c}{\tau^2} \right) \partial_\alpha^{-1} \mathbb{P} \\ \bar{\gamma}c \left( \frac{\bar{\gamma}}{\tau^2} - \frac{cAM}{\pi\tau^2} \right) \partial_\alpha^{-1} \mathbb{P} + \frac{cM^2 Ag}{\pi^2 \tau^2} \partial_\alpha^{-2} H & c \left( \frac{A\bar{\gamma}}{\tau^2} - \frac{cM}{\pi\tau^2} \right) \partial_\alpha^{-1} H \end{bmatrix}.$$

For  $\partial_\tau L(\mu)$ , however, it is perhaps more helpful to note the equality

$$\partial_\tau L(\mu) = -\frac{1}{\tau} (L(\mu) - \text{Id}).$$

Since we know that  $L(\mu_*)v_i = 0$  for  $i \in \{1, 2\}$ , this tells us immediately that

$$\partial_\tau L(\mu_*)v_i = \frac{1}{\tau} v_i.$$

We next compute  $\partial_c L(\mu)v_i$ , and letting  $j \in \{k, \ell\}$  be as appropriate,

$$\partial_c L(\mu)v_i = \left[ - \left( \frac{\tilde{\gamma}^2 \pi}{\tau c M j} - \frac{2\tilde{\gamma}A}{\tau} \cdot \frac{1}{j} - \frac{M A g}{c \pi \tau} \cdot \frac{1}{j^2} - \frac{A\tilde{\gamma}}{\tau} \cdot \frac{1}{j} + \frac{2cM}{\pi \tau} \cdot \frac{1}{j} \right) \cos(j\alpha) \right].$$

Then, taking the projection, we have

$$\begin{aligned} \Pi_k \partial_c L(\mu_*)v_1 &= \frac{\pi}{\langle \phi_k, \phi_k \rangle} \left( \left( \tau k M + cM \left( A\tilde{\gamma} - \frac{cM}{\pi} \right) \right) \left( \frac{-\tilde{\gamma}A\pi + cM}{cM\tau k} \right) \right. \\ &\quad \left. + \left( \frac{-A\tilde{\gamma}\pi + cM}{cM\tau k} \right) \left( \tilde{\gamma}^2 \pi - 3cM\tilde{\gamma}A - \frac{M^2 A g}{\pi k} + \frac{2c^2 M^2}{\pi} \right) \right) \\ &= \frac{\pi}{\langle \phi_k, \phi_k \rangle} \left( \frac{-A\tilde{\gamma}\pi + cM}{cM\tau k} \right) \\ &\quad \times \left( \tau k M + \frac{c^2 M^2}{\pi} + \tilde{\gamma}^2 \pi - \frac{M^2 A g}{\pi k} - 2cM\tilde{\gamma}A \right). \end{aligned}$$

Similarly, we have

$$\begin{aligned} \Pi_\ell \partial_c L(\mu_*)v_2 &= \frac{\pi}{\langle \phi_\ell, \phi_\ell \rangle} \left( \frac{-A\tilde{\gamma}\pi + cM}{cM\tau \ell} \right) \\ &\quad \times \left( \tau \ell M + \frac{c^2 M^2}{\pi} + \tilde{\gamma}^2 \pi - \frac{M^2 A g}{\pi \ell} - 2cM\tilde{\gamma}A \right). \end{aligned}$$

We next compute

$$\begin{aligned} \Pi_k \partial_\tau L(\mu_*)v_1 &= \frac{\pi}{\langle \phi_k, \phi_k \rangle} \left( \left( -\frac{\pi}{\tau c M} \right) \left( \tau k M + cM \left( A\tilde{\gamma} - \frac{cM}{\pi} \right) \right) + \frac{1}{\tau} (-cM + A\tilde{\gamma}\pi) \right) \\ &= \frac{\pi}{\langle \phi_k, \phi_k \rangle} \left( -\frac{\pi k}{c} \right), \end{aligned}$$

and the corresponding formula

$$\begin{aligned} \Pi_\ell \partial_\tau L(\mu_*)v_2 &= \frac{\pi}{\langle \phi_\ell, \phi_\ell \rangle} \left( \left( -\frac{\pi}{\tau c M} \right) \left( \tau \ell M + cM \left( A\tilde{\gamma} - \frac{cM}{\pi} \right) \right) + \frac{1}{\tau} (-cM + A\tilde{\gamma}\pi) \right) \\ &= \frac{\pi}{\langle \phi_\ell, \phi_\ell \rangle} \left( -\frac{\pi \ell}{c} \right). \end{aligned}$$

**Acknowledgements** The authors thank the anonymous referee for many helpful suggestions which have improved the manuscript. The first author acknowledges support from the Air Force Office of Scientific Research and the Joint Directed Energy Transition Office. The second author is grateful to the National Science Foundation for support through grant DMS-2307638.

**Author Contributions** D.M.A. proposed the work and carried out mathematical analysis. B.F.A. designed numerical methods, carried out numerical simulations, prepared all figures, and placed the work in its appropriate context with respect to prior literature. Both authors prepared and edited the manuscript, and both authors reviewed the final manuscript.

**Data Availability** No datasets were generated or analyzed during the current study.

## Declarations

**Conflict of interest** The authors declare no competing interests.

**Open Access** This article is licensed under a Creative Commons Attribution 4.0 International License, which permits use, sharing, adaptation, distribution and reproduction in any medium or format, as long as you give appropriate credit to the original author(s) and the source, provide a link to the Creative Commons licence, and indicate if changes were made. The images or other third party material in this article are included in the article's Creative Commons licence, unless indicated otherwise in a credit line to the material. If material is not included in the article's Creative Commons licence and your intended use is not permitted by statutory regulation or exceeds the permitted use, you will need to obtain permission directly from the copyright holder. To view a copy of this licence, visit <http://creativecommons.org/licenses/by/4.0/>.

## References

1. Akers, B., Ambrose, D.M., Wright, J.D.: Traveling waves from the arclength parameterization: vortex sheets with surface tension. *Interfaces Free Bound.* **15**(3), 359–380 (2013)
2. Akers, B., Nicholls, D.P.: Wilton ripples in weakly nonlinear dispersive models of water waves: existence and analyticity of solution branches. *Water Waves* **3**(1), 25–47 (2021)
3. Akers, B., Nicholls, D.P.: Wilton ripples in weakly nonlinear models of water waves: existence and computation. *Water Waves* **3**(3), 491–511 (2021)
4. Akers, B.F., Ambrose, D.M., Pond, K., Wright, J.D.: Overturned internal capillary-gravity waves. *Eur. J. Mech. B Fluids* **57**, 143–151 (2016)
5. Akers, B.F., Ambrose, D.M., Sulon, D.W.: Periodic traveling interfacial hydroelastic waves with or without mass. *Z. Angew. Math. Phys.* **68**(6), Paper No. 141 (2017)
6. Akers, B.F., Ambrose, D.M., Sulon, D.W.: Periodic travelling interfacial hydroelastic waves with or without mass II: multiple bifurcations and ripples. *Eur. J. Appl. Math.* **30**(4), 756–790 (2019)
7. Akers, B.F., Ambrose, D.M., Wright, J.D.: Gravity perturbed Crapper waves. *Proc. R. Soc. Lond. Ser. A Math. Phys. Eng. Sci.* **470**(2161), 20130526 (2014)
8. Akers, B.F., Reeger, J.A.: Three-dimensional overturned traveling water waves. *Wave Motion* **68**, 210–217 (2017)
9. Akers, B.F., Seiders, M.: Numerical simulations of overturned traveling waves. In: *Nonlinear Water Waves—An Interdisciplinary Interface*, Tutor. Sch. Workshops Math. Sci., pp. 109–122. Birkhäuser/Springer, Cham (2019)
10. Ambrose, D.M.: Well-posedness of vortex sheets with surface tension. *SIAM J. Math. Anal.* **35**(1), 211–244 (2003) (**electronic**)
11. Ambrose, D.M., Masmoudi, N.: The zero surface tension limit of two-dimensional water waves. *Commun. Pure Appl. Math.* **58**(10), 1287–1315 (2005)
12. Ambrose, D.M., Strauss, W.A., Wright, J.D.: Global bifurcation theory for periodic traveling interfacial gravity-capillary waves. *Ann. Inst. H. Poincaré C Anal. Non Linéaire* **33**(4), 1081–1101 (2016)
13. Baker, G., Nachbin, A.: Stable methods for vortex sheet motion in the presence of surface tension. *SIAM J. Sci. Comput.* **19**(5), 1737–1766 (1998)

14. Baker, G.R., Meiron, D.I., Orszag, S.A.: Generalized vortex methods for free-surface flow problems. *J. Fluid Mech.* **123**, 477–501 (1982)
15. Baldi, P., Toland, J.F.: Bifurcation and secondary bifurcation of heavy periodic hydroelastic travelling waves. *Interfaces Free Bound.* **12**(1), 1–22 (2010)
16. Chabane, M., Choi, W.: On resonant interactions of gravity-capillary waves without energy exchange. *Stud. Appl. Math.* **142**(4), 528–550 (2019)
17. Constantin, A., Strauss, W., Vărvăruță, E.: Global bifurcation of steady gravity water waves with critical layers. *Acta Math.* **217**(2), 195–262 (2016)
18. Ehrnström, M., Escher, J., Wahlén, E.: Steady water waves with multiple critical layers. *SIAM J. Math. Anal.* **43**(3), 1436–1456 (2011)
19. Ehrnström, M., Johnson, M.A., Maehlen, O.I.H., Remonato, F.: On the bifurcation diagram of the capillary-gravity Whitham equation. *Water Waves* **1**(2), 275–313 (2019)
20. Friedrich, O., Sonar, T.: Regularising discretizations of the Birkhoff–Rott equation. *Math. Methods Appl. Sci.* **18**(8), 615–625 (1995)
21. Hou, T.Y., Lowengrub, J.S., Shelley, M.J.: Removing the stiffness from interfacial flows with surface tension. *J. Comput. Phys.* **114**(2), 312–338 (1994)
22. Hou, T.Y., Lowengrub, J.S., Shelley, M.J.: The long-time motion of vortex sheets with surface tension. *Phys. Fluids* **9**(7), 1933–1954 (1997)
23. Langer, R., Trichtchenko, O., Akers, B.: Wilton ripples with high-order resonances in weakly nonlinear models. *Water Waves* **6**, 97–126 (2024)
24. Mæhlen, O., Seth, D.S.: Asymmetric travelling wave solutions of the capillary-gravity Whitham equation (2023). arXiv preprint [arXiv:2312.15343](https://arxiv.org/abs/2312.15343)
25. Martin, C.I., Matic, B.-V.: Existence of Wilton ripples for water waves with constant vorticity and capillary effects. *SIAM J. Appl. Math.* **73**(4), 1582–1595 (2013)
26. Plotnikov, P.I., Toland, J.F.: Modelling nonlinear hydroelastic waves. *Philos. Trans. R. Soc. Lond. Ser. A Math. Phys. Eng. Sci.* **369**(1947), 2942–2956 (2011)
27. Părău, E., Dias, F.: Interfacial periodic waves of permanent form with free-surface boundary conditions. *J. Fluid Mech.* **437**, 325–336 (2001)
28. Wilkening, J., Zhao, X.: Spatially quasi-periodic water waves of infinite depth. *J. Nonlinear Sci.* **31**(3), Paper No. 52 (2021)
29. Wu, S.: Well-posedness in Sobolev spaces of the full water wave problem in 2-D. *Invent. Math.* **130**(1), 39–72 (1997)
30. Zakaria, K.: Wilton ripples between two uniform streaming magnetic fluids. *Int. J. Non-Linear Mech.* **39**(6), 1051–1066 (2004)